JOURNAL OF MATERIALS SCIENCE 11 (1976) 1807–1816

A DTA study of zone-refined $LiRF_4$ (R=Y, Er)

J. S. ABELL, I. R. HARRIS
Department of Physical Metallurgy and Science of Materials, University of Birmingham, UK
B. COCKAYNE, J. G. PLANT
Royal Radar Establishment, Malvern, Worcs, UK

The melting behaviour of zone-refined bars of $LiYF_4$ and $LiErF_4$ has been investigated by means of differential thermal analysis (DTA). Both compounds can be produced congruently under an atmosphere of carefully purified argon. Consideration of the constitutional variations occurring along the length of the bars has established that the congruent melting composition is non-stoichiometric, and a detailed analysis of the profiles of the thermal events indicates that both compounds possess a homogeneity range and are not line compounds as previously reported. The influence of purity on the melting behaviour is assessed and the implication of the results on the crystal growth of laser materials based on these compounds is discussed.

Introduction

Recently, there has been considerable discussion about the melting behaviour of the compounds $LiYF_4$ (LYF) and $LiErF_4$ (LEF) and related compounds which has stemmed largely from the use of this group of materials as solid state laser host lattices emitting radiation at 2.06 μm when doped with Ho^{3+} and sensitized with Tm^{3+} [1]. Much of the argument has been concerned with the problem of whether these compounds melt congruently or in a peritectic manner, and the role of impurities in determining the melting behaviour. Gabbe and Harmer [2] suggest that LYF is a peritectic phase, which agrees with the $LiF–YF_3$ phase diagram of Thoma *et al.* [3] reproduced in Fig. 1, whilst Pastor *et al.* [4] report that LYF is conguently melting provided that the melting takes place in an environment containing HF. Better agreement exists for LEF which is generally accepted to be congruently melting [5] as depicted in Fig. 1, but even here, Pastor and Robinson [6] have shown that the allotropic phase change normally present in the ErF_3 component, can be removed by the presence of HF.

The work described here, which forms part of a study of the phase relationships existing in the $LiF–YF_3–ErF_3$ system, has used differential thermal analysis (DTA) to study the precise nature

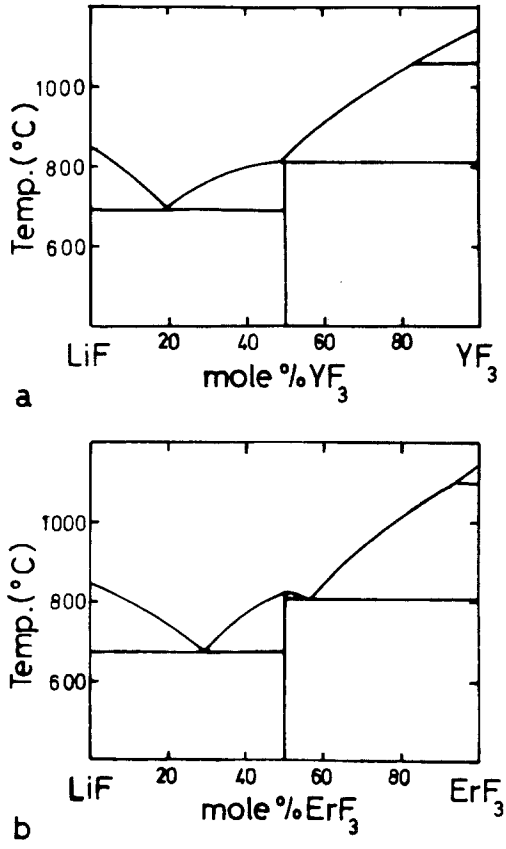

Figure 1 Reported phase diagrams for the $LiF-YF_3$ and $LiF-ErF_3$ systems, including the compounds of $LiYF_4$ (LYF) and $LiErF_4$ (LEF).

of the melting reactions in zone-refined bars of LYF and LEF produced as starting material for the Czochralski growth of compounds with the general formula $LiY_{1-x}Er_xF_4$ $(0 \ll x \ll 1)$. The results have also enabled the phase relationships in the immediate neighbourhood of the two compounds to be established and the influence of purity to be evaluated. The implication of these factors on the crystal growth of the more complex fluoride laser compounds is discussed.

2. Experimental

The zone-refining apparatus for preparing the bars studied here has been described elesewhere [7]. The component fluorides were supplied by BDH Ltd as optran grade material. The LiF was in the form of crystalline chips whilst the rare earth fluorides were in powdered form which was either used directly as untreated material or heat-treated in an atmosphere containing HF at 800° C. The appropriate fluorides mixed in stoichiometric proportions to make LYF and LEF were first melted and subsequently subjected to the single passage of a molten zone. The melt was contained in a vitreous carbon boat under an atmosphere of argon, flowing at a rate of 200 cm^3 min^{-1}. The argon had been carefully purified with respect to residual water vapour and oxygen by passing it through a molecular sieve and over titanium heated to 700° C. The initial zone width was approximately 2.5 cm and the rate of traverse was 6 mm h^{-1}.

X-ray powder diffraction patterns were recorded on a standard 114 mm diameter Debye-Scherrer camera using filtered Cr$K\alpha$ radiation. Differential thermal analyses were performed on a Linseis L62 DTA incorporating Pt/Pt–Rh thermocouples and tantalum crucibles with tight-fitting lids. Powder samples weighing 0.01 g and a standard heating rate of either 2 or 10° C min^{-1} were employed so that a direct comparison of the DTA profiles could be made for each sample. Strict control of the specimen weight and the heating rate through the melting reactions was particularly necessary because observation of subtle changes in the DTA profiles was required in order to characterize the detailed constitutional variations occurring in these fluorides.

Prior to each experiment the equipment was evacuated to 2×10^{-5} Torr and flushed with commercial purity argon (typical impurities $O_2 - 5$, $N_2 - 20$, $H_2O - 4$, CO, CO_2, H_2, H/C all < 1, in volumes per million). The DTA tests were conducted under a static atmosphere of this argon, except where further purification was achieved by passing the gas through a molecular sieve to remove water vapour. Thermal events on both heating and cooling were recorded but temperatures derived from the heating data were regarded as more significant since undercooling was observed. Temperatures were taken, by convention, to be the point of deviation from the baseline as shown in Fig. 2, and temperature resolution was assessed to be ± 2° C. Differences in the DTA profiles and their dependence on constitution and thermal history have been analysed by means of measurement of such parameters as peak height and half-peak breadth of the profiles as illustrated in Fig. 2.

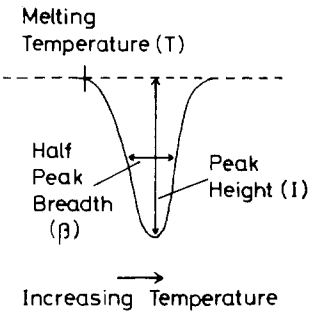

Figure 2 Schematic representation of a DTA profile illustrating the parameters used to characterize variations in melting behaviour.

3. Results

3.1. Examination of starting constituents

Samples of LiF, YF_3 and ErF_3 which had been used in the preparation of the zone-refined bars were examined in the DTA equipment. Both RF_3 samples revealed two high temperature endotherms, one corresponding to the orthorhombic–hexagonal transition, the other to the melting reaction. For YF_3, the solid state transition occurred at 1065° C with melting at 1150° C, while in the case of ErF_3 the corresponding temperatures were 1090 and 1125° C. LiF melted congruently at 845° C.

3.2. Comparison of LYF and LEF bars

Several zone-refined bars of each compound, prepared from starting materials heat-treated in HF, were examined. One bar of each compound was also prepared from untreated constituents. Three distinct regions could be identified in each bar as

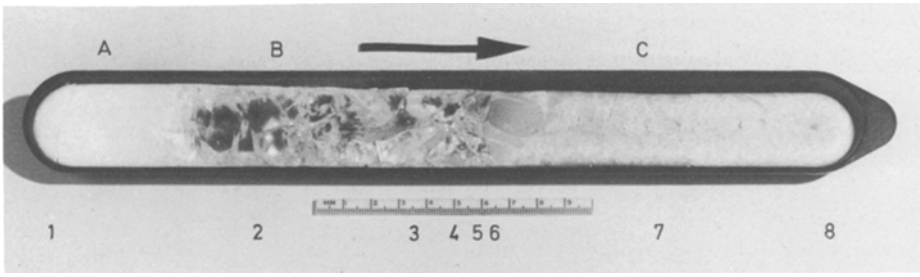

Figure 3 Micrograph of a LYF zone-refined bar with the three main regions A, B, C identified. The numbers refer to the samples tested by DTA and reported in Section 3.3.

shown in Fig. 3. The first material to solidify (A) is translucent due to its small-grained structure. The central region (B) consists of large transparent grains, whilst the last material to solidify (C) is completely opaque. With HF-treated constituents, the central region B formed 50 to 60% of the total volume of the bar whilst in untreated material the volume of clear crystal was frequently as small as 5 to 10%. There was no apparent difference in the optical quality of the central region for the two compounds LYF and LEF. At the end of the zoning process a white deposit was always observed on the exit plate of the refining chamber.

Powder samples were prepared from each of the regions A, B and C. The X-ray diffraction patterns of all the samples exhibited lines characteristic of the Scheelite-type, b c t structure [8] except those for region C in the LYF bar which had extra lines corresponding to LiF. The pattern taken from the white deposit consisted solely of LiF lines.

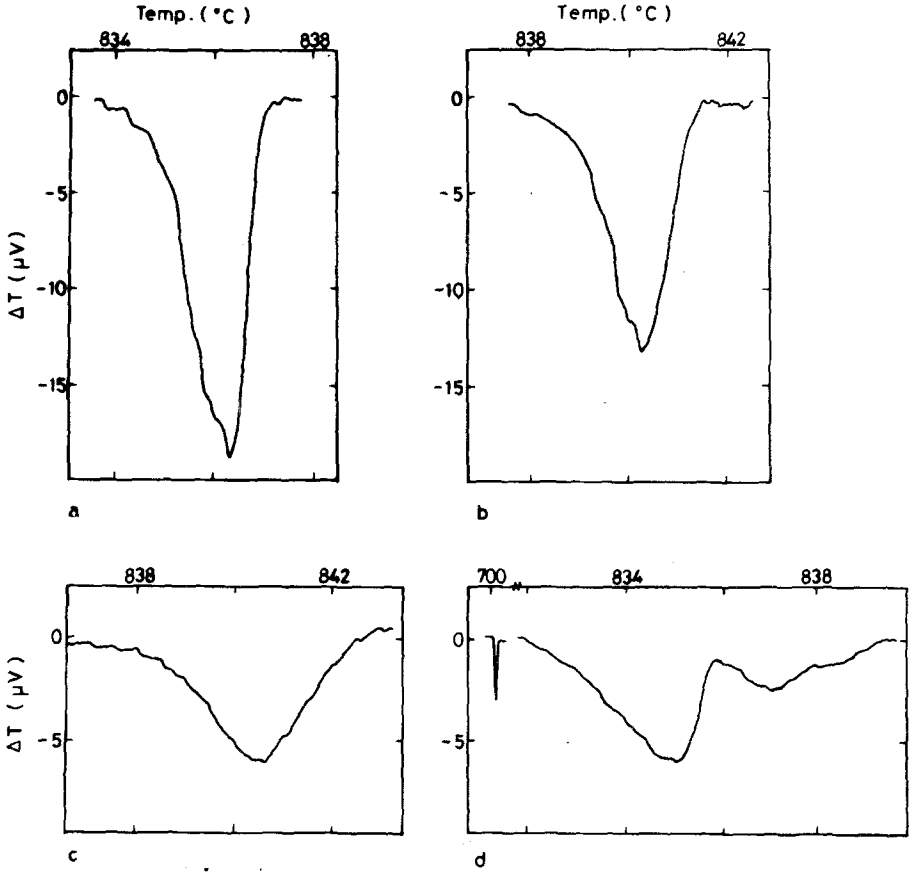

Figure 4 DTA profiles recorded at a heating rate of 2° C min^{-1} on samples taken from various regions of the zone-refined bars, (a) LYF section B, (b) LEF section B, (c) LEF section B close to interface with section C and (d) LYF section C (untreated constituents).

The DTA profiles recorded on the powdered, clear crystal regions indicated a close similarity in the solidification behaviour for LYF and LEF. Both revealed sharp single peak endotherms characteristic of congruently melting compounds as shown in Fig. 4a and b. The LYF peak area is larger than that for LEF indicating a higher latent heat of fusion for the yttrium compound. The optical clarity of the bars was reduced in that part of region B immediately adjacent to C, and this is reflected in the DTA profiles (Fig. 4c) which are broad and of relatively low intensity.

A-type regions also showed essentially single peak reactions, although less intense and often broader than the corresponding B-region profiles. In contrast, the samples from section C revealed different thermograms, consisting of a sharp endotherm at $\sim$ 700° C, corresponding to the eutectic existing between LiF and LYF or LEF, followed by a liquidus reaction in the region of 800° C. For LYF, the eutectic reaction was strong with a fairly weak liquidus reaction, whereas for LEF the eutectic reaction was much smaller and that of the liquidus correspondingly larger. This shows that the last region of LYF to solidify is richer in LiF than the corresponding LEF region, thus confirming the X-ray powder diffraction data.

Samples taken from the LYF bar prepared from untreated constituents showed generally similar behaviour except that the sample taken from the last portion to solidify showed a eutectic plus a double peak melting reaction as shown in Fig. 4d. However, it should be re-emphasized that the extent of the regions A and B are very much reduced in these bars.

3.3. Constitutional variations along an LYF bar

The previous section has shown quite clearly that DTA profiles are an extremely sensitive means of studying the constitutional variations associated with crystal quality in these mixed fluoride materials. A systematic investigation of the DTA profiles of samples taken from various points along the length of a zone-refined bar of LYF was undertaken in order to characterize the detailed constitutional variations occurring during the zoning process. LYF was chosen in preference to LEF for this study because of the wider variation in melting reaction behaviour reported for this compound [3, 4].

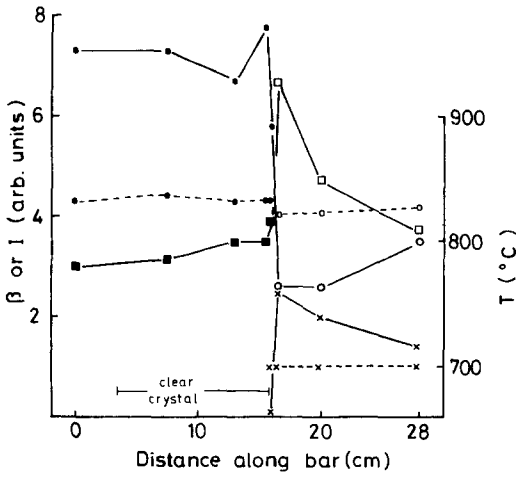

Figure 5 Diagrammatical representation of various parameters associated with the thermal events measured on samples 1 to 8 taken from different regions along the zone-refined LYF bar of Fig. 3.

Key:

Event	Intensity	Breadth	Temperature
Congruent	●—●	■—■	●——●
Liquidus	o—o	□—□	o——o
Eutectic	X — X		X——X

Eight samples from the bar in Fig. 3 were tested, sample 1 from region A, 2 to 4 from region B, 5 and 6 from either side of the sharp interface between B and C, and 7 and 8, are widely spaced samples from region C. The parameters measured from the thermal events recorded for these samples are plotted in Fig. 5. Samples 1 to 4 showed similar single peak endotherms typified by Fig. 6a, with the peak breadth increasing slightly with distance along the bar. The measured melting temperature for these samples was in the range 831 to 837° C. Sample 5 showed a reduced intensity and enhanced breadth, as depicted in Fig 6b. An extremely weak eutectic reaction was also detected in this sample; this is only just intense enough to be represented on Fig. 5. However, just across the interface in sample 6, a much stronger eutectic reaction was recorded followed by a broad diffuse liquidus at 822° C (Fig. 6c). Samples 7 and 8 gave similar thermograms to 6, but with a significant reduction in the eutectic reaction and a corresponding increase in intensity and sharpness of the liquidus reaction. An associated rise in liquidus reaction temperature from 822 to 828° C also occurred progressively between samples 6 and 8. For comparison the thermogram recorded on sample 8 is shown in Fig. 6d.

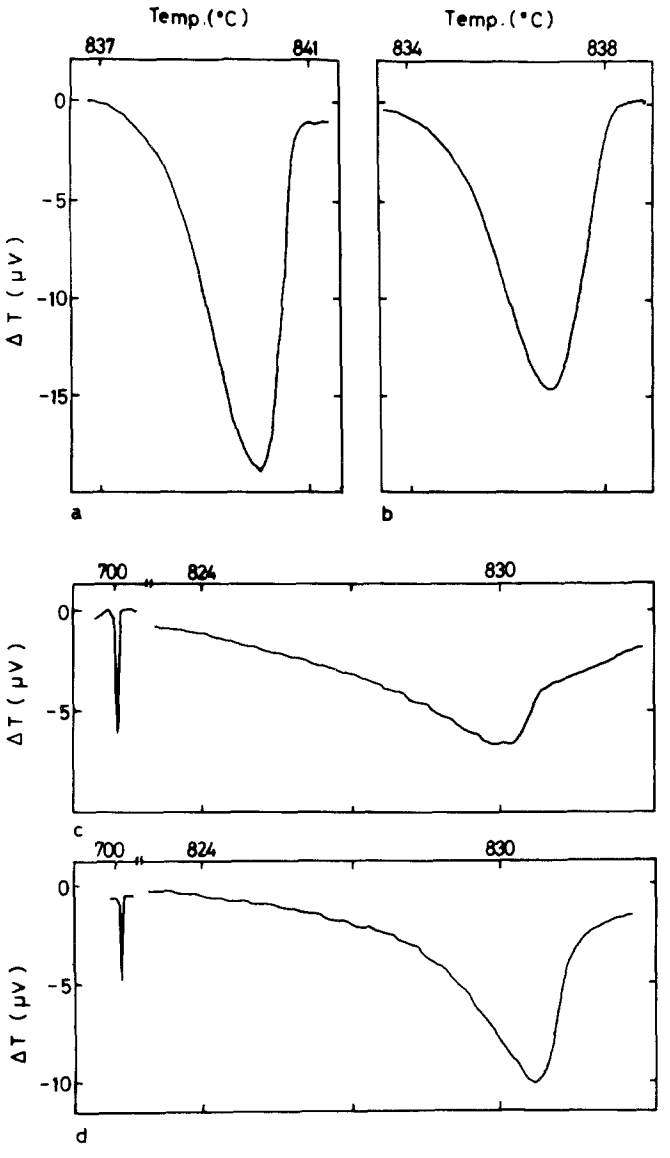

Figure 6 DTA profiles recorded on samples taken from the LYF bar in Fig. 3, (a) sample 3 (2° C min^{-1}), (b) sample 5 (2° C min^{-1}), (c) sample 6 (eutectic 10° C min^{-1}, liquidus 2° C min^{-1}) and (d) sample 8 (eutectic 10° C min^{-1}, liquidus 2° C min^{-1}).

3.4. Effects of thermal cycling

The effect of thermal cycling on the nature of the melting reaction for both LYF and LEF was used to study the influence of environmental contamination on the constitution of these compounds. These experiments were performed *in situ* in the DTA apparatus using samples from the clear crystal sections (B) of a zone-refined bar of each compound. The cycling was carried out under the same static atmosphere of commercial purity argon.

In both compounds, the sharp profile observed on the first cycle was broadened and reduced in intensity on a subsequent cycle as shown in Fig. 7. The maximum broadening was observed on this second cycle, but further cycling produced a decrease in the profile breadths. The parameters derived from these profiles are plotted in Fig. 7e. No significant broadening was detected in a LYF clear crystal sample which had previously been heated in air to 600° C for $1\frac{1}{2}$ h. In none of these samples was the eutectic reaction recorded, either on heating or cooling. However, a sample of LYF which had previously been re-melted in a 70% argon–30% air mixture did show a eutectic reaction; this was followed by a double peak melting reaction very similar to that obtained on LYF prepared from untreated constituents (Fig. 4d). On cycling this sample the eutectic reaction was no longer detected and a broad single

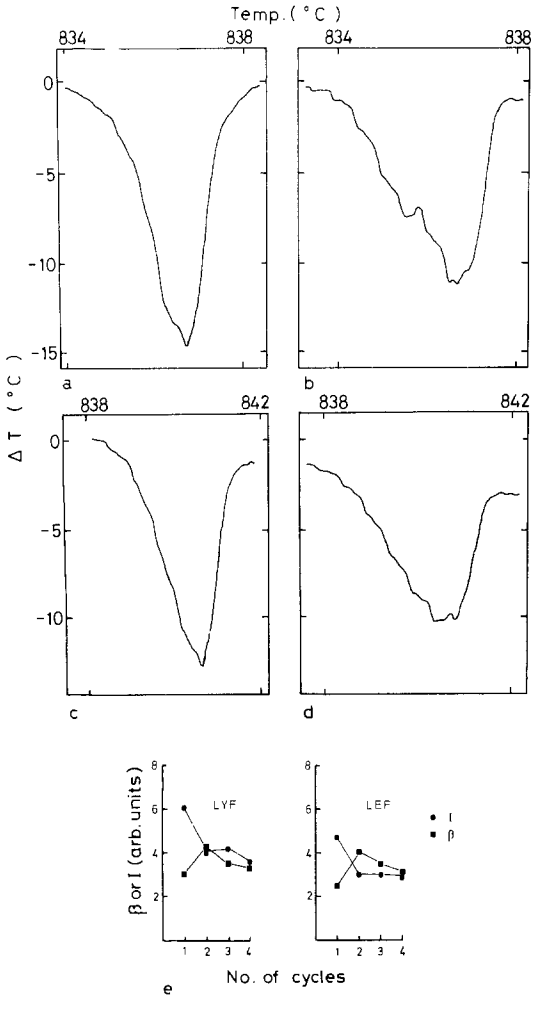

Figure 7 The effect of thermal cycling on the DTA profiles of the clear section B of a LYF bar during (a) the first cycle, (b) the second cycle and the same section of an LEF bar during (c) the first cycle and (d) the second cycle. In (e) the parameters peak intensity (I) and half-peak breadths (β) on each cycle are represented.

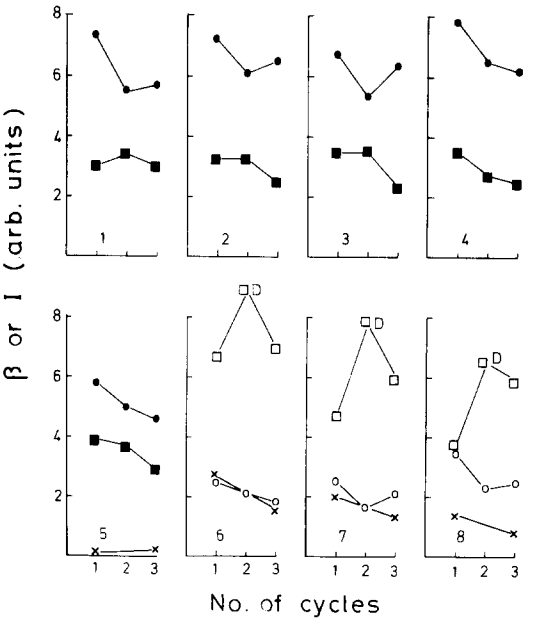

Figure 8 The parameters peak intensity (I) and half-peak breadth (β) measured for the DTA profiles during thermal cycling of samples 1 to 8 taken from the LYF bar in Fig. 3. Key is the same as for Fig. 5 with D indicating a double peak profile.

melting reaction was observed over the same temperature range as the original double profile. Essentially similar behaviour was observed on thermally cycling samples from region C of a zone-refined bar of LYF prepared from untreated constituents.

The effect of thermal cycling on the DTA profiles of the eight samples taken from the LYF bar is shown diagrammatically in Fig. 8. For these experiments the argon atmosphere was purified further by passing through a molecular sieve to remove the small traces of water vapour present in commercial purity argon. Comparison of Fig. 8 (samples 1 to 5) with Fig. 7e (samples tested under untreated argon) shows that the removal of water vapour almost eliminates the peak broadening on the second cycle. In samples 6 to 8, where the eutectic is detected, the already broad liquidus broadens even more on the second cycle displaying a double peak which subsequently becomes unresolvable on a further cycle. During this process, the eutectic intensity is significantly reduced for all three samples.

3.5. Crystal growth

Single crystals of both LYF and LEF have been produced by the Czochralski technique using as the starting charge the zone-refined material which gave single peak DTA reactions; the details of the growth procedure and apparatus are described elsewhere [7]. No additions of LiF were found necessary for the production of clear scatter-free crystals and no HF was used in the growth atmosphere at any stage. This clearly establishes that both LYF and LEF are congruently melting compounds.

4. Discussion

The observation of similar single peak endotherms for the clear crystalline regions of both LYF and LEF zone-refined bars, together with the sub-

sequent growth of clear single crystal LYF by the Czochralski method from zone-refined starting material, without the addition of excess LiF, constitutes firm evidence for the congruency of both phases. LEF has always been reported as congruent [5], but LYF was thought to be formed by a peritectic reaction [2, 3] until recent work showed that under a carefully controlled atmosphere containing HF, LYF could be produced congruently [4]. The implication of that work is that the reported peritectic nature of LYF is associated with impurites and that the HF atmosphere is necessary to purge the melt of these impurities. Use of a similar, carefully controlled atmosphere has enabled the high temperature phase transition in ErF_3 to be eliminated and crystals of the orthorhombic phase have been produced directly from the melt [6]. A similar suppression of this transition in YF_3 has not been reported.

In the present work, the use of argon purified by passing through a molecular sieve and over heated titanium was found to be entirely satisfactory in producing large clear crystals of both compounds, provided that the constituent RF_3's were heat-treated in HF prior to compound formation; under these conditions HF was not required during zone-refining or crystal growth.

The difference in these observations could be accounted for by the initial purity of the constituent fluorides and/or the purity of the gas atmosphere. Our observation in both YF_3 and ErF_3 of a reaction corresponding to the high temperature orthorhombic–hexagonal transition, previously shown to be suppressed for ErF_3 in an HF growth atmosphere [6], would imply that our starting material was not as pure as that used by Pastor *et al.* [4]. Hence, the purity of the gas atmosphere appears to be the major factor in accounting for the difference.

The thermograms of the opposite ends of the zone-refined bars clearly show that the lack of transparency arises from two distinct effects. The translucence due to the formation of a small grained structure at the front end results from multiple nucleation which occurs in the absence of a seed crystal, whilst the opacity of the rear portion of the bars is due to the two-phase eutectics consisting of either LYF or LEF and LiF.

Since the starting composition of the melt for both compounds is 50 mol % LiF:50 mol % RF_3, the segregation of LiF to the back end of the bars and the depostion of excess LiF on the exit plate of the zone-refiner establishes that the congruent composition is non-stoichiometric. This LiF segregation implies that the congruent melting point lies to the RF_3-rich side of the stoichiometric composition. It is difficult to estimate the congruent composition accurately because a composition variation exists in the LiF-rich end of the bars, as shown in Fig. 5. Using the liquidus temperatures from this figure in conjunction with the phase diagram* of Thoma *et al.* [3] (Fig. 1a), an average composition of 53 LiF:47 YF_3 may be assigned to section C of the LYF bar. Assuming the composition of the remainder of the bar is invariant, a congruent composition of 48 LiF:52 YF_3 can be derived. This neglects the LiF deposited on the exit plate of the refining chamber thus making an estimate of the YF_3 content somewhat low.

An analysis of the experimentally observed DTA profiles indicates that a homogeneity range exists for both compounds. For instance, the broadened and double liquidus profiles of Figs. 4, 6 and 7 can be attributed to the finite solidus–liquidus separation which would exist for compositions within this homogeneity range but away from the congruent point. Incorporation of this homogeneity range in a possible phase diagram in the region of LYF is shown in Fig. 9. Sample 5 of the LYF bar shows a broad liquidus together with an extremely small eutectic reaction thus implying a composition to the LiF-rich side of congruency consistent with the segregation of LiF to this end of the bar. It is this co-existence of a small eutectic reaction and a broad liquidus which determines the shape of the LYF homogeneity range in the region of the LiF–LYF eutectic isotherm.

Further evidence for the existence of the homogeneity range is provided by the thermal cycling experiments on samples 6 to 8 of the LYF bar. The decrease in intensity of the eutectic reaction and the associated change of the liquidus profile (Fig. 8) can be accounted for by the loss of LiF, which progressively changes the composition from that corresponding to a eutectic outside the LYF range to compositions involving the solidus–liquidus separation existing within the homogeneity range, according to the scheme outlined in

*While this phase diagram is not strictly applicable to the present congruently melting material, the liquidus is changing shape so slowly in this region that the resultant error will be slight.

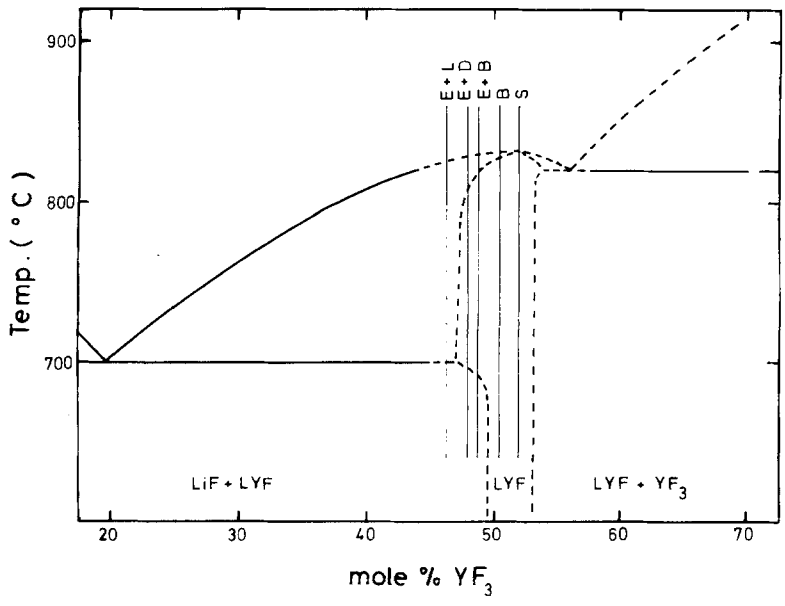

Figure 9 Proposed phase relationships in the region of LYF on the LiF-YF_3 system. The vertical solid lines correspond to distinct melting bahaviour, observed by DTA, which have been used to construct the dotted phase boundaries.
Key: E + L = eutectic + liquidus
E + D = eutectic + double peak
E + B = eutectic + broad peak
B = broad peak
S = single peak (congruent)

Fig. 9. The disappearance of the eutectic reaction on cycling the 70% Ar/30% air re-melt sample provides a further example of the occurrence of LiF-loss in these materials and is consistent with the above scheme.

The eutectic point between LYF and YF_3 in Fig. 9 is drawn in accordance with the work of Pastor *et al.* [4] who, from their crystal growth studies, deduced a eutectic composition corresponding to a YF_3: LiF molar ratio of $r = 1.28$ which is equivalent to 56 mol % YF_3. Their observation that single crystal growth was possible from a melt of composition $r = 1.069$ ($\equiv 51.7$ mol % YF_3) can now be explained in terms of the non-stoichiometric congruent composition and associated homogeneity range for LYF deduced from the present work.

The thermal cycling experiments can also be used to understand the effect of contamination on the melting reactions of these compounds. Thermal cycling of clear crystal in untreated argon produces broad liquidus peaks indicating that contamination induces a departure from congruency; cycling in purer argon gives no such broadening. The extreme contamination experienced by the sample re-melted in a 70% Ar/30% air atmosphere yields the eutectic reaction associated with LiF–rich compositions. The small proportion of clear crystal in the zone-refined bars prepared from untreated constituents also implies that contamination moves the melt composition away from the congruent point; the majority of these bars are opaque and again exhibit the eutectic reaction.

A detailed understanding of the effects induced by contamination may require consideration of a quaternary system but, in any event, the present results are consistent with an association between contamination and a change in composition to the LiF-rich side of stoichiometry. Such a change could be achieved by several possible routes: the formation of an oxyfluoride based on RF_3, the selective oxidation of the R component to R_2O_3, or by the reaction of R with OH^- ions by means of hydrolysis. All these processes will selectively remove RF_3 from the melt yielding the observed composition shift. Whatever reaction is responsible, the present cycling experiments have shown that water vapour is a necessary factor.

The occurrence of contamination effects such as broad and double peak liquidi have probably lead to the previous assignment of a peritectic nature to LYF but are more properly associated with incongruency within the LYF homogeniety

range. It should be noted that, in the work of Pastor *et al.* [4], the observation of a second endotherm on their thermograms at $\sim 700^\circ$ C, while indicating a departure from congruency, cannot be interpreted in terms of the onset of a peritectic nature for LYF, as these authors imply. As the present work has shown, this additional reaction corresponds to the eutectic isotherm existing between LiF and LYF and not the apparent peritectic between LYF and YF_3 ($\sim 810^\circ$ C). The detection of what appears to be a double peak profile at $\sim 830^\circ$ C in their thermograms is more significant to the departure from congruency; this was not explained previously but can now be readily interpreted in terms of the proposed phase diagram (Fig. 9).

The identification of these two competing processes, namely contamination and LiF-loss, enables the variety of melting reactions observed in this work to be explained once the non-stoichiometric congruent point and associated homogeneity range have been established. For instance, the peak broadening and subsequent sharpening (Fig. 7e) can be explained by contamination followed by LiF-loss, effectively changing the composition in opposite senses. LiF-loss also determines the composition profile existing in section C of the LYF bar (Fig. 5). As solidification proceeds, segregation of LiF to the molten zone and loss of LiF from the zone occurs. Initially, with a small well-defined zone, the former predominates and the zone become progressively richer in LiF; a corresponding drop in melting temperature occurs so that, for a constant power input, the zone volume increases. Eventually the composition of the molten zone becomes so LiF-rich that solidification within the LYF range is no longer possible and a two-phase opaque eutectic forms. At this stage LiF segregation stops and the molten zone becomes large enough ($\sim 40\%$ of total ingot length) for the associated LiF losses to be significant; subsequent solidification of this section becomes less rich in LiF with the resultant composition gradient indicated in Fig. 5.

So far, no attempt has been made to zone-refine a melt of the congruent composition of Fig. 9 to see if the proportion of clear material can be increased. Such an improvement would not necessarily be achieved because the excess LiF may play a significant role in the purification of the melt that occurs in the zoning process. Certainly, LiF seems to play such a role in the Stockbarger growth of $LiY_{0.5}Er_{0.5}F_4$ crystals where single crystals have not yet been obtained without excess LiF [9]. The presence of excess LiF in a contaminated melt may assist removal of contaminants thereby allowing the majority of the bar to crystallize congruently. However, the growth of a LYF single crystal by the Czochralski technique from clear zone-refined material demonstrates that excess LiF is unnecessary provided that subsequent contamination of the melt is avoided.

Clearly, DTA is a very sensitive means of determining not only the constitution of the different regions produced by the zone-refining process, but also the subtle variations in crystal quality occurring in the predominantly clear crystalline region. A departure from a sharp single peak profile associated with congruency can be successfully correlated with a decrease in the optical quality of the material produced. A similar correlation between optical quality and DTA profile has been observed in a single crystal of $LiY_{0.5}Er_{0.5}F_4$ grown by the Stockbarger method [10]. It should be emphasized that detection of these subtle changes in peak profiles has only been possible by using a slow heating rate of 2° C min^{-1} through the melting reactions, compared with the 20° C min^{-1} used by Pastor *et al.* [4] which necessarily obscures the fine detail of the profiles.

The technological significance of the present work is that large clear crystals of congruently melting LYF and LEF can be produced, and that this can be achieved under an atmosphere which is relatively easy to obtain, namely carefully purified argon. The availability of such material has enabled single crystals of LYF and LEF to be grown by the Czochralski technique under the same atmosphere.

It is, however, compositions in the $LiY_{1-x}Er_xF_4$ system which are of particular interest for their lasing properties. Since it can now be seen that the two end components are both congruent, a finite solidus–liquidus separation must exist across the sytem. Obviously the extent of this separation will play an important role in determining the quality of crystalline material produced by zone-refining and Czochralski growth at these intermediate compositions. However, defects due to the segregation associated with the solidus–liquidus separation need no longer be obscured by the effects arising from contami-

nation and non-congruent melting which have been clearly identified by the present investigation.

Acknowledgement

This work was carried out with the support of Procurement Executive, Ministry of Defence.

References

1. E. P. CHICKLIS, C. S. NAIMAN, R. C. FOLWEILER, D. R. GABBE, H. P. JENSEN and A. LINZ, *Appl. Phys. Letters* **19** (1971) 119.
2. D. GABBE and A. L. HARMER, *J. Crystal Growth*, **3**, **4** (1968) 544.
3. R. E. THOMA, C. F. WEAVER, H. A. FRIEDMAN, H. INSLEY, L. A. HARRIS and H. A. YAKEL, *J. Phys. Chem.* **65** (1961) 1096.
4. R. C. PASTOR, M. ROBINSON and W. M. AKUTAGAWA, *Mat. Res. Bull.* **10** (1975) 501.
5. R. E. THOMA, *Prog. Sci. Tech. Rare Earths* **2** (1966) 110.
6. R. C. PASTOR and M. ROBINSON, *Mat. Res. Bull.* **9**. (1974) 569.
7. B. COCKAYNE and J. G. PLANT, to be published.
8. G. KELLER and H. SCHMUTZ, *J. Inorg. Nucl. Chem.* **27** (1965) 900.
9. D. A. JONES, B. COCKAYNE, R. A. CLAY and P. A. FORRESTER, *J. Crystal Growth* **30** (1975) 21.
10. B. COCKAYNE, D. A. JONES, J. S. ABELL and I. R. HARRIS, *J. Crystal Growth* in press.

Received 4 March and accepted 22 March 1976.